Thermodynamics of the Glucocorticoid Receptor–DNA Interaction: Binding of Wild-Type GR DBD to Different Response Elements†

Thomas Lundbäck,‡,§ Carol Cairns,‡,∥ Jan-Ake Gustafsson,∥ Jan Carlstedt-Duke,∥ and Torleif Härd*,§

Center for Structural Biochemistry and Department of Medical Nutrition, Karolinska Institutet, NOVUM, S-141 57 Huddinge, Sweden

Received December 7, 1992; Revised Manuscript Received February 9, 1993

ABSTRACT: We used fluorescence spectroscopy to study the chemical equilibria between an 82-residue protein fragment containing the core conserved region of the glucocorticoid receptor DNA-binding domain (GR DBD) and a palindromic glucocorticoid response element (GRE), a consensus GRE half-site, a consensus estrogen response element (ERE) half-site, and two intermediate half-sites (GRE2 and ERE2). Equilibrium parameters were determined at 20 °C and buffer conditions that approximate intracellular conditions. The association constants for GR DBD binding to the GRE (5′TGTTCT3′) and GRE2 (5′TGTCCT3′) half-sites at 85 mM NaCl, 100 mM KCl, 2 mM $MgCl_2$, and 20 mM Tris-HCl at pH 7.4 and low concentrations of an antioxidant and a nonionic detergent are $(1.0 \pm 0.1) \times 10^6$ M^{-1} and $(5.1 \pm 0.2) \times 10^5$ M^{-1}, respectively. The association constants for binding to the ERE (5′TGACCT3′) and ERE2 (5′TGATCT3′) half-sites are $<10^5$ M^{-1}. The implications of these numbers for the specificity and affinity for the binding of the intact GR to DNA are discussed. Comparison of GR DBD binding to a GRE half-site and a palindromic GRE sequence allowed us to estimate the cooperativity parameter, $\omega_{obs} = 25$–50, for GR DBD binding to GRE. The thermodynamics of the GR DBD interaction with a GRE half-site were also investigated by determining the temperature dependence of the observed association constant. The nonlinear dependence in ln K_{obs} as a function of $1/T$ is consistent with a change in standard heat capacity, $\Delta C_p°_{obs} = 1.0 \pm 0.2$ kcal mol^{-1} K^{-1}. The binding process is shown to be entropy driven at temperatures <26 °C and enthalpy driven at temperatures >35 °C. The thermodynamics of the binding process are consistent with dehydration of nonpolar surfaces upon formation of the complex, although the observed $\Delta C_p°_{obs}$ cannot be fully accounted for by this mechanism.

Noncovalent interactions between DNA and DNA-binding proteins (transcription factors) that recognize specific DNA sequences play central roles in molecular biology. The structures of several DNA–protein complexes have been determined using X-ray crystallography and nuclear magnetic resonance [see Pabo and Sauer (1992) for a recent review]. These structures have in many cases revealed intermolecular interactions (hydrogen bonds and hydrophobic and electrostatic contacts) that might contribute to the sequence specificity. A commonly accepted notion is that specific interactions between functional groups on the interacting DNA and protein surfaces act to stabilize the sequence-specific complexes by contributing to the enthalpy component (ΔH) of the free energy of binding. However, the underlying physical chemistry of sequence-specific DNA binding of proteins is not completely understood. Studies on a few systems have shown that specific as well as nonspecific DNA–protein associations might be entropy-driven (Record et al., 1991; Ha et al., 1989; Bulsink et al., 1985, Takeda et al., 1992), i.e., that the change in entropy (ΔS) upon formation of the complex contributes significantly to the binding constant, and that the enthalpy term in some cases even counteracts the binding process. A large positive change in entropy might result from the release of ions and water molecules from individual macromolecular surfaces upon association of DNA and proteins (Record et al., 1991, and references therein). The observed intermolecular interactions might in these cases be the result of a perfect surface complementarity, causing an optimal release of water and counterions upon binding. On the other hand, a sequence-specific complex formed with $\Delta H > 0$ might still be stabilized by interactions contributing to ΔH as long as ΔH for binding to a specific site is less than ΔH for nonspecific binding, i.e., $\Delta\Delta H < 0$ for the process (nonspecific complex) ⇒ (sequence-specific complex).

These considerations motivate a complete characterization of the thermodynamics of each studied system before drawing conclusions about the relative contributions of various interactions that can be observed in a structure of a DNA–protein complex. Structural and thermodynamic studies should also be carried out in combination with protein mutagenesis and studies of binding to various DNA binding site sequences in order to dissect and explore the effects of adding and/or removing various functional groups on the interacting surfaces.

We are employing this approach in our studies of the DNA-binding domain of the glucocorticoid receptor (GR DBD),[1] through which the effects of glucocorticoids are mediated. The glucocorticoid receptor is a member of the family of nuclear hormone receptors, which includes the receptors for other steroid hormones (such as the estrogen receptor, ER), thyroid hormones, retinoic acid, and vitamin D_3 [see Evans (1988) for a review]. The binding of ligand to the GR induces

† This work was supported by the Swedish Natural Sciences Research Council (Grant Nos. K-KU 8593-309 and S-FO 8593-308), the Swedish Medical Research Council (Grant Nos. 2819 and 8998), and the Swedish Research Council for Engineering Sciences.

* Author to whom correspondence should be addressed.
‡ To be considered as equal first authors.
§ Center for Structural Biochemistry.
∥ Department of Medical Nutrition.

[1] Abbreviations: GR DBD, glucocorticoid receptor DNA-binding domain; GRE, glucocorticoid response element; ER, estrogen receptor; ERE, estrogen response element; bp, base pair; CT DNA, calf thymus DNA; DTT, dithiothreitol; $C_{12}E_8$, octaethylene glycol monododecyl ether.

0006-2960/93/0432-5074$04.00/0

a transformation such that it translocates to the nucleus and associates with DNA to regulate transcriptional activity. The DNA-binding sites for the GR are termed glucocorticoid response elements (GREs) and usually consist of 15 base pair (bp) partially palindromic sequences comprising two half-sites with a 3 bp intervening gap (Beato, 1989). Estrogen response elements (EREs) differ in only one or two central base pairs per half-site (Strähle et al., 1987), when compared to the GREs. The GR DBD binds as a dimer to the GRE sequence, with initial binding preferentially occurring to one of the two half-sites. Previous occupancy of this high-affinity binding site has been shown to facilitate the binding to the second half-site (Tsai et al., 1988; Härd et al., 1990a). This facilitated binding is dependent on the distance between the half-sites and their relative orientation but is not dependent on the integrity of the DNA backbone (Dahlman-Wright et al., 1990). This is consistent with a two-site cooperative model where DNA binding is dependent not only on protein interactions with the DNA but also on interactions between the two protein molecules. The region of the protein responsible for the protein–protein interactions has been identified genetically (Dahlman-Wright et al., 1991) and structurally (Luisi et al., 1991).

The structures of the GR DBD (Härd et al., 1990b) and the ER DBD (Schwabe et al., 1990) have been solved using NMR spectroscopy, and a structure of a dimeric complex of GR DBD bound to DNA has been solved using X-ray crystallography (Luisi et al., 1991). Three amino acid residues (G458, S459, and V462 in the rat GR) in the GR and ER DBDs have been identified as crucial for the discrimination between GRE and ERE sequences (Danielsen et al., 1989; Mader et al., 1989; Umesono & Evans, 1989). Since the response elements differ in only two base pairs per half-site, it has been suggested that the three identified residues interact directly with these base pairs. However, in the crystal structure of the GR DBD–GRE complex only one specific contact (originating from V462) was found (Luisi et al., 1991). Substitution of the three GR residues with the corresponding ER residues might result in one or two direct interactions, and this could account for the sequence discrimination. Extensive genetic studies have subsequently yielded information about positive and negative determinants among the three residues (Zilliacus et al., 1992), but these data are not easily interpreted in terms of intermolecular interactions. It is clear that further structural studies as well as characterization of the thermodynamics of the DBD–DNA equilibrium as outlined above is necessary for a complete understanding of sequence specificity in this system.

The present paper represents the second in a series of studies aimed at a complete understanding of the thermodynamics of the GR DBD–DNA interaction. We previously showed that fluorescence spectroscopy can be used to monitor this equilibrium due to the quenching of tyrosine fluorescence when GR DBD binds to DNA (Härd et al., 1990a). We investigated the differences between sequence-specific and nonspecific binding at various salt concentrations, and we were able to estimate the product between the cooperativity parameter and the average association constant (ωK) for GR DBD binding to a naturally occurring GRE sequence at high (570 mM) monovalent cation concentrations. In this study we focus on the sequence-specific binding at buffer conditions that more closely resemble those found in the interior of a typical mammalian cell (Alberts et al., 1983). The objectives of the present work are the following: (i) to quantitatively determine the association constants for binding of GR DBD to various GRE and ERE response element half-sites (Figure 1), without interference from non-specific binding; (ii) to estimate the contribution from cooperative binding by comparing binding to a half-site to that to an idealized GRE with two identical half-sites arranged as inverted repeats; (iii) to investigate the thermodynamics for GR DBD binding to a GRE half-site by means of a van't Hoff analysis, i.e., by examining the temperature dependence of the observed equilibrium constant.

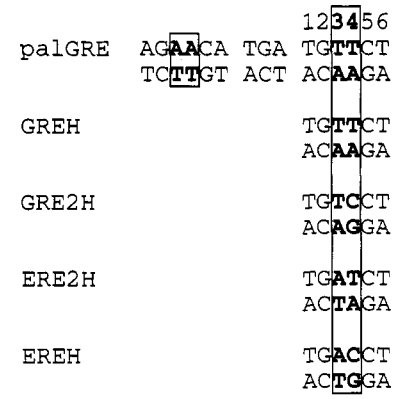

FIGURE 1: Glucocorticoid and estrogen response elements used in this study. The hexameric GREH and EREH half-sites differ in only two central base pairs (denoted 3 and 4). The GRE2H and ERE2H thus represent intermediate binding sites containing both GRE and ERE specific base pairs. The palGRE is an idealized GRE with two identical half-sites arranged as inverted repeats. These sequences are incorporated in DNA oligomers as described under Materials and Methods.

MATERIALS AND METHODS

Protein Purification. The GR DBD (amino acid residues Leu420–Ile500 of the human GR + an N-terminal methionine) was expressed in *Escherichia coli* and purified as described elsewhere (Berglund et al., 1992), with the following modifications. *E. coli* cells were grown in Luria broth medium containing 1% casamino acids, 1% glucose, 50 μg/mL ampicillin, and 30 μg/mL chloramphenicol. After elution from the FPLC column (Pharmacia Mono S), the protein was dialyzed against a buffer containing 50 mM NaCl, 1 mM DTT (dithiothreitol), and 50 mM Tris-HCl at pH 7.4. [All solutions were prepared using deionized (Milli-Q) and autoclaved water.] Sequence-specific DNA-binding activity was checked by gel retardation analysis as described by Tsai et al. (1988). Stock solution concentrations of GR DBD were determined spectrophotometrically using the extinction coefficient ϵ_{280nm} = 4200 M^{-1} cm^{-1} calculated for tyrosine absorption (Cantor & Schimmel, 1980). Some stock solution concentrations were also determined using a Bradford protein assay (Bio-Rad). The two methods yielded results that agreed within 25%. All concentrations quoted below refer to spectrophotometric determinations.

Synthesis and Purification of DNA. Synthetic DNA oligomers were used for equilibrium studies of specific binding. The GRE, GRE2, ERE, and ERE2 binding half-sites (Figure 1) were incorporated in 32 base pair (bp) DNA oligomers, and the palindromatic GRE sequence was incorporated in a 41 bp oligomer. The oligomer sequences were selected so that no half-site GRE/ERE-like sequences were created (Dahlman-Wright et al., 1990) and so that the oligomer sequences flanking the half-sites were identical. All DNA oligomers were purified using high-pressure liquid chromatography. Following purification, complementary strands were annealed in equal amounts, as determined by the

absorbance at 260 nm, in 150 mM NaCl and 10 mM Tris-HCl at pH 7.4. Calf thymus (CT) DNA was purchased from Sigma (type I) and dissolved by mild shearing in 150 mM NaCl and 10 mM Tris-HCl at pH 7.4. The solution was then repeatedly extracted with an equal volume of phenol/$CHCl_3$ (ratio 1:1) until protein contaminants were removed as checked for by measuring an absorbance ratio $A_{260}/A_{280} > 1.8$. The CT DNA was then precipitated with ethanol, resuspended in 150 mM NaCl and 10 mM Tris-HCl at pH 7.4, and dialyzed against this buffer. All DNA concentrations were determined spectrophotometrically using an average extinction coefficient ϵ_{260nm} = 13 200 M (base pairs)$^{-1}$ cm^{-1} (Mahler et al., 1964).

Steady-State Fluorescence Measurements. All fluorescence measurements were carried out in 85 mM NaCl, 100 mM KCl, 2 mM $MgCl_2$, 1 mM DTT, 0.1 mM $C_{12}E_8$ (octaethylene glycol monododecyl ether purchased from Fluka), and 20 mM Tris-HCl at pH 7.4. The nonionic detergent ($C_{12}E_8$) was used to prevent protein adhesion to quartz and plastic surfaces. Background fluorescence due to this detergent was found to be negligible. Steady-state fluorescence was measured on a Shimadzu RF-5000 spectrofluorometer equipped with a 150-W Xenon arc lamp, using fluorescence cells with inner dimensions of 3 × 3 mm. The excitation wavelength was 280 nm with a 3-nm bandwidth, and emission spectra were recorded between 290 and 320 nm with an emission monochromator bandwidth of 10 nm. The intensity at 304 nm, corresponding to the emission maximum, was used when calculating binding isotherms. The measured intensity was corrected for background emission and Raman light scattering from water by subtracting signals from DNA + buffer samples. The fluorescence intensities at high DNA concentrations were also corrected for optical filtering effects (Birdsall et al., 1983). Reabsorption of light emitted from the protein at 304 nm was estimated to be negligible. The temperature of the cell compartment was controlled using a Shimadzu constant temperature cell holder connected to an LKB 2209 circulating water bath. The temperature could be controlled with an accuracy of ±1 °C within the range 10–35 °C.

Equilibrium Titrations. Titrations were performed as reverse titrations, in which different amounts of DNA were added at a constant protein concentration. Before titration, the sample and the titrant were allowed to reach thermal equilibrium in the water bath. The titrant was added to the cuvette using a micropipette, and the emission spectrum was recorded three times in order to minimize the effects of instrumental fluctuations. The excitation shutter was closed between measurements in order to minimize photochemical degradation of the protein. Upon examination with continuous illumination, no photobleaching could be observed during the time scale used for equilibrium titrations.

The fractional fluorescence quenching (Q_{obsd}) was calculated as $(I_o - I)/I_o$, where I_o is the protein fluorescence intensity observed in the absence of DNA and I is the intensity in the presence of DNA. Binding isotherms are presented as plots of Q_{obsd} against the logarithm of the DNA oligomer concentration (Figures 3, 4, and 6). Each titration was carried out three times to improve the precision in Q_{obsd} and to allow determination of experimental errors (estimated standard deviations).

Analysis of Binding Isotherms. Theoretical binding isotherms were fitted directly to the observed fluorescence quenching using a simple one-site equilibrium model for GR DBD binding to DNA oligomers containing GRE half-sites (GREH and GRE2H) or a two-site cooperative model (Härd et al., 1990a) for binding to the palindromic GRE (palGRE) (Figure 1). It is not necessary to consider dimerization of uncomplexed DBD molecules, because the equilibrium titrations were carried out at low (0.6 μM) concentrations, whereas NMR studies on this protein strongly suggest that it is still predominantly monomeric at much higher (1 mM) concentrations (Härd et al., 1990c; Berglund et al., 1992). The derivation of the theoretical binding isotherms is described in the Supplementary Material. Since the thermodynamic quantities estimated in this study are based on the total macromolecular concentrations only, neglecting nonideality of the solution, the parameters evaluated will be valid only at the conditions specified. This is indicated by the subscript "obs" throughout the paper. The concentration of GR DBD bound to DNA (C_b) was calculated as $C_b = (Q_{obsd}/Q_{max})C_{tot}$, where C_{tot} is the total GR DBD concentration and Q_{max} is the maximum quenching, that is, the quenching observed when all the protein in the sample is bound to DNA. It is important to note that the observed quenching, Q_{obsd}, is not proportional to the concentration of bound protein, C_b, if different binding modes result in different fluorescence quantum yields. In the present study, this scenario might apply for binding to the palindromic GRE sequence (palGRE), if the fluorescence quantum yield for a complex with a single DBD is different from that of two cooperatively bound DBD molecules. However, in our previous study we showed that this is not the case (Härd et al., 1990a).

Nonlinear least-squares fits of the equilibrium parameters to measured equilibrium data were carried out using MATLAB for Macintosh. A minimizing function based on the Nelder–Meade simplex algorithm was used to minimize the χ^2 merit function

$$\chi^2 = \sum_{i=1}^{N} \left\{ \frac{Q(i) - Q_{obsd}(i)}{\text{std } Q_{obsd}(i)} \right\}^2 \quad (1)$$

where $Q(i)$ and $Q_{obsd}(i)$ are the calculated and observed fluorescence quenching at titration point i, respectively, std $Q_{obsd}(i)$ is the standard deviation of the observed quenching, and N is the number of data points. Errors in the best-fit equilibrium parameters were determined using Monte Carlo simulations (Press et al., 1986): several "synthetic" data sets (typically 20–50) were generated for each titration by drawing random numbers from normal distributions with means corresponding to Q_{obsd} and standard deviations equal to the experimental errors obtained at each point (std Q_{obsd}). The minimization was then carried out for each set of synthetic data, and standard deviations in the optimized parameters were calculated. These numbers correspond to experimental standard errors as long as the shapes of the distribution functions for repeated experimental determinations of the equilibrium parameters are similar to the probability distributions for repeated observations of the "true" equilibrium parameters (Press et al., 1986).

RESULTS

Binding to Half-Site Containing DNAs. Equilibrium titrations of GR DBD with the five DNA oligomers (Figure 1) at 20 °C are shown in Figure 3. The results indicate that the affinities to the various half-sites decrease in the order GRE > GRE2 > ERE2 ≈ ERE in good agreement with previous results from gel shift studies (Zilliacus et al., 1991). A precise determination of Q_{max}, i.e., the GR DBD fluorescence quantum yield in the bound state, is desirable for accurate determinations of the equilibrium parameters. At the present

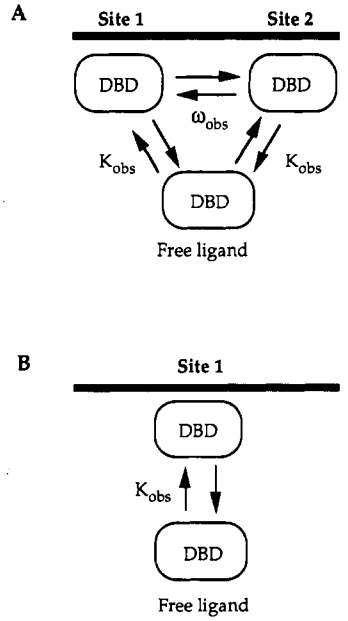

FIGURE 2: (A) Two-site cooperative model for binding of GR DBD to an idealized GRE with identical half-sites at high salt concentrations, where nonspecific DNA-binding is negligible. K_{obs} is the association constant for binding to site 1 and 2 and ω_{obs} represents the cooperativity parameter. (B) The corresponding one-site model for binding of GR DBD to a half-site GRE. The theoretical binding isotherms expected for these models are derived in the Supplementary Material.

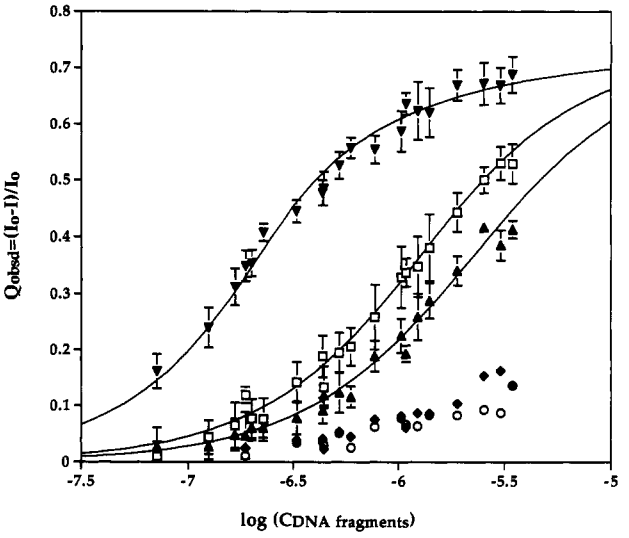

FIGURE 3: Fractional fluorescence quenching as a function of DNA concentration for reverse titrations of GR DBD with (▼) palindromic GRE, (□) GREH, (▲) GRE2H, (○) ERE2H, and (◆) EREH at constant protein concentration (0.6 μM). The curves represent the best fit of theoretical binding isotherms to experimental data with Q_{max} values according to Table I. All titrations were performed in 85 mM NaCl, 100 mM KCl, 2 mM $MgCl_2$, 1 mM DTT, 0.1 mM $C_{12}E_8$, and 20 mM Tris-HCl at pH 7.4 and a temperature of 20 °C. Data points represent the averages with estimated standard deviations of three separate titrations.

buffer conditions, which were chosen in order to minimize nonspecific binding, the titrations with the half-site DNAs could not be carried out until maximum quenching was observed, i.e., until the curves level off at $Q = Q_{max}$. The highest DNA concentration that could be used was limited by the absorbance of the DNA bases at 280 nm, which severely attenuates the excitation light intensity. A titration at slightly lower salt concentrations was therefore carried out to determine Q_{max}. This titration shows a binding curve that levels off at $Q_{max} = 0.73$ at 20 °C (Figure 4). The temperature was also

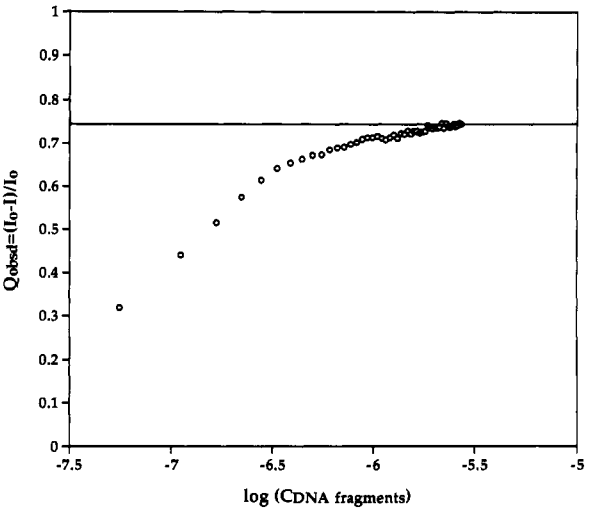

FIGURE 4: Fractional fluorescence quenching as a function of DNA concentration for reverse titrations of GR DBD with GREH at 20 °C and constant protein concentration (0.6 μM). The line represents the maximum fractional quenching, $Q_{max} = 0.73$. The titrations were performed in 100 mM NaCl, 1 mM $MgCl_2$, 1 mM DTT, 0.1 mM $C_{12}E_8$, and 10 mM Tris-HCl at pH 7.4.

Table I: Temperature Dependence of the Maximum Quenching, Q_{max}

temp (°C)	10	12.5	15	20	25	30	35
Q_{max}	0.78	0.77	0.76	0.73	0.74	0.74	0.74

varied within the range 10–35 °C for the starting and the end points of this titration to determine the temperature dependence in Q_{max} (Table I). It is possible that nonspecific complexes with a higher fluorescence quantum yield (Härd et al., 1990a) contribute to the observed quenching in titrations performed at lower salt concentrations. This effect of nonspecific binding can be seen in the beginning of the titration curve shown in Figure 4, where the observed quenching could not possibly be due to specific binding only. However, at the endpoint of the low-salt titration there is a 5-fold excess of specific binding sites over GR DBD molecules in the solution, resulting in a predominance of specific complexes. Furthermore, the Q_{max} value obtained in the titration with GREH at the lower salt concentration agrees very well with the Q_{max} observed in the titration with palGRE at higher salt concentrations (Q_{max} = 0.70–0.75; Figure 3) as well as with the previously determined $Q_{max} = 0.72$ (Härd et al., 1990a).

It is not directly evident from the plots in Figure 3 that the equilibria involve binding to a single DNA site and no nonspecific binding. However, a comparison of the binding to GRE with that of ERE2 shows that a single base pair mutation within the GRE half-site (in the 32 bp DNA oligomers) significantly reduces the binding affinity, suggesting that binding occurs primarily at the GRE half-site. Furthermore, binding stoichiometries of 0.7–1.9 GR DBD molecules per DNA oligomer were extracted from Benesi Hildebrand plots (Marshall, 1978) for GR DBD binding to GREH at temperatures between 10 and 35 °C (one of these plots is shown in Figure 5). Nonspecific binding is also expected to be very weak at the present salt concentrations (Härd et al., 1990a). A simple 1:1 stoichiometry for GR DBD binding to half-site GRE sequences has also been concluded from gel shift experiments carried out at salt concentrations lower then those used here (Dahlman et al., 1990). We therefore feel that it is safe to conclude that the fluorescence quenching observed with the GREH and GRE2H DNA oligomers reflect the binding of a single GR DBD

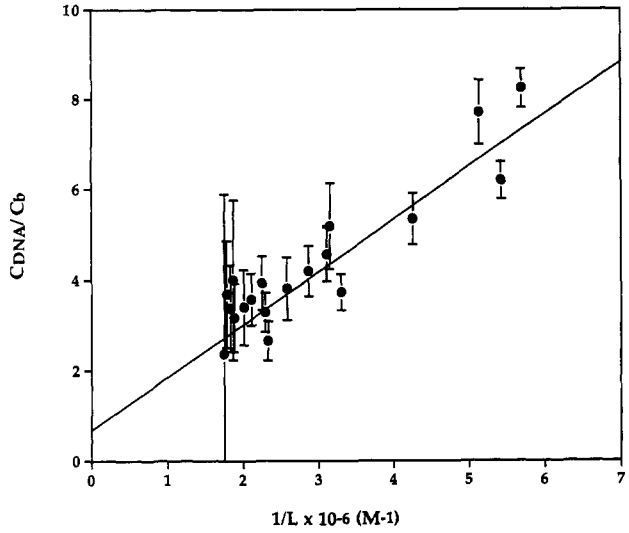

FIGURE 5: Benesi–Hildebrand plot for the equilibrium between GR DBD and GREH at 35 °C. C_{DNA} is the total concentration of DNA oligomers, C_b is the concentration of GR DBD bound to DNA calculated using Q_{max} = 0.74, and [L] is the free GR DBD concentration. Buffer conditions are the same as those given in the legend to Figure 3. The curve represents the best fit of the binding isotherm (Marshall, 1978) to experimental data and extrapolates to a binding stoichiometry of 1.46 Gr DBDs per DNA oligomer.

molecule to a GRE half-site.

The best-fit association constants, with uncertainties estimated from Monte Carlo simulations, for GR DBD binding to the GREH and GRE2H are listed in Table II together with corresponding free energies of association ($\Delta G°_{obs} = -RT \ln K_{obs}$). The fits were carried out treating both the association constant, K_{obs}, and the maximum quenching, Q_{max}, as unknown variables as well as keeping Q_{max} fixed (Q_{max} = 0.73 from Table I) and fitting the association constant only. The latter case yielded association constants $K_{obs} = (1.0 \pm 0.1) \times 10^6$ M^{-1} and $(5.1 \pm 0.2) \times 10^6$ M^{-1} (Table II).

GR DBD binding to the EREH and ERE2H half-sites is much weaker than binding to the GREH and GRE2H half-sites (Figure 3), as expected. The titration curves obtained with EREH and ERE2H are in fact not very different from that obtained with nonspecific CT DNA (not shown), suggesting that nonspecific as well as specific binding might contribute to the observed quenching. These equilibria could therefore not be treated using the simple one-site model. Furthermore, the measured data do not allow a fit to a more general model, because the titration curves do not span a sufficient range of the complete binding isotherm. However, the maximum quenching for nonspecific binding is not expected to be very different from that of specific binding (Härd et al., 1990a). Based on this fact, the one-site model with Q_{max} = 0.73 can be used to obtain a rough estimate of the maximum possible association constant for the binding of GR DBD to the EREH and ERE2H oligomers at the present conditions [$K_{obs} < (1.0 \pm 0.2) \times 10^5 M^{-1}$]. The differences in free energies for binding to the various half-sites at 20 °C are shown in Table III.

Binding to a Palindromic GRE. The GR DBD binding affinity for the full GRE sequence (palGRE) is stronger than binding to the half-sites, as expected (Figure 3), due to the presence of two half-sites in this sequence and the effects of cooperative binding (Härd et al., 1990a). The data were fitted to the theoretical binding isotherm treating the binding constant, K_{obs}, and the cooperativity parameter, ω_{obs}, as variables and fixing Q_{max} = 0.72. The latter assumption is in this case well justified by experimental data, since the observed quenching clearly levels off at high DNA concentrations. The optimized parameters were $K_{obs} = (8.4 \pm 5.0) \times 10^5$ M^{-1} and $\omega_{obs} = (1.5 \pm 2.4) \times 10^2$. The large uncertainities reflect the high correlation between K_{obs} and ω_{obs}, i.e., it is equally easy to fit a large value of ω_{obs} together with a small value of K_{obs}, and conversely. Fitting ω_{obs} when keeping K_{obs} fixed to the value determined for binding to the GRE half-site ($K_{obs} = 1.0 \times 10^6$ M^{-1}) gives an optimized $\omega_{obs} = 30 \pm 3$, and keeping K_{obs} fixed to $K_{obs} = 8.4 \times 10^5$ M^{-1} obtained in the two-parameter fit above results in $\omega_{obs} = 45 \pm 3$. These fittings were also performed treating Q_{max} as an unknown parameter, which resulted in Q_{max} values between 0.71 and 0.73 and no significant differences in the cooperativity parameter. Given these results, we conclude that the association constant for binding to one of the two half-sites in a full GRE sequence is not very different from the association constant for binding to an isolated GRE half-site and that the cooperativity parameter for dimeric binding of GR DBD to GRE is in the order of ω_{obs} = 25–50.

Thermodynamic Analysis of GR DBD Binding to GREH. The temperature dependence of the binding of GR DBD to GREH is illustrated in Figure 6. The binding affinity is clearly reduced at temperatures <15 °C and actually shows a small decrease also at temperatures >30 °C. In these experiments, the pH value of the experimental buffer varied between 7.2 (at 35 °C) and 7.8 (at 10 °C). The pH dependency of the binding of GR DBD to GREH at 20 °C was therefore examined, but no significant change in binding could be observed within the relevant pH range, indicating that the observed effects were not due to a variation in pH with temperature. Binding constants were determined as described above for the case of GR DBD binding to GREH and GRE2H at 20 °C, and the results are summarized in Table II.

The temperature dependence of the association constant of the GR DBD–GREH equilibrium is also presented as a van't Hoff plot with ln K_{obs} versus $1/T$ (Figure 7A). The van't Hoff plot is nonlinear due to a negative change in standard heat capacity, $\Delta C_p°_{obs}$, upon formation of the complex. This results in compensating enthalpic and entropic contributions to the standard free energy change. In this case, the temperature dependence of K_{obs} can be expressed as

$$\ln K_{obs} = (\Delta C_p°_{obs}/R)[(T_H/T) - \ln(T_S/T) - 1] \quad (2)$$

where T_H and T_S are the temperatures at which $\Delta H°_{obs} = 0$ and $\Delta S°_{obs} = 0$, respectively, and where $\Delta C_p°_{obs}$ is assumed to be temperature independent over the temperature range investigated. A value of $\Delta C_p°_{obs} = -1.0 \pm 0.2$ kcal mol^{-1} K^{-1} was estimated from a three-parameter fit of eq 2 to the data in Figure 7A, using Monte Carlo simulations to estimate the error (standard deviation) in the optimized value. The optimized values of T_H and T_S were 26 and 35 °C, respectively. The estimated temperature dependencies in $\Delta H°_{obs}$ and $\Delta S°_{obs}$ [calculated according to Ha et al. (1989)] are shown in Figure 7B together with $\Delta G°_{obs}$ obtained from experimental data. The change in standard free energy varies only slightly within the investigated temperature range. In contrast, the enthalpy and entropy effects involved show strong but opposite dependencies upon temperature, balancing the change in free energy.

DISCUSSION

The objectives of the present study were to (1) quantitatively determine the equilibrium constant for binding of GR DBD to various GRE and ERE half-sites without interference from nonspecific binding; (2) estimate the contribution from

Table II: Best-Fit Parameters for Sequence-Specific GR DBD–DNA Equilibra[a]

		optimized K_{obs} for measured Q_{max}[b]	simultaneously optimized K_{obs} and Q_{max}[c]			
response element	temp (°C)	K_{obs} ($M^{-1} \times 10^{-6}$)	K_{obs} ($M^{-1} \times 10^{-6}$)	Q_{max}	$\Delta G°$ obs[d] (kcal mol^{-1})	ω_{obs}
GREH	10	0.49 ± 0.04	0.6 ± 0.2	0.77 ± 0.14	−7.4 ± 0.1	
	12.5	0.58 ± 0.03	0.8 ± 0.2	0.69 ± 0.07	−7.5 ± 0.1	
	15	0.89 ± 0.05	1.0 ± 0.2	0.73 ± 0.04	−7.8 ± 0.1	
	20	1.03 ± 0.08	1.3 ± 0.3	0.69 ± 0.06	−8.1 ± 0.1	
	25	0.97 ± 0.08	1.2 ± 0.3	0.69 ± 0.05	−8.2 ± 0.1	
	30	1.05 ± 0.09	1.0 ± 0.2	0.78 ± 0.07	−8.3 ± 0.1	
	35	0.93 ± 0.06	1.0 ± 0.3	0.71 ± 0.07	−8.4 ± 0.1	
GRE2H	20	0.5 ± 0.1	0.5 ± 0.1	0.79 ± 0.08	−7.7 ± 0.1	
ERE2H	20	<1.0 ± 0.1			−6.7 ± 0.1	
EREH	20	<1.0 ± 0.1			−6.7 ± 0.1	
palGRE	20	0.8 ± 0.5				nd
		1.0			−8.1	30 ± 3[e]
		0.8			−7.9	45 ± 3[f]

[a] Uncertainties represent estimated standard deviations. [b] Optimized using Q_{max} values given in Table I. [c] Optimized with Q_{max} treated as an unknown parameter. [d] Calculated from K_{obs} values optimized for measured Q_{max}. [e] Optimized for $K_{obs} = 1.0 \times 10^6$ M^{-1}. [f] Optimized for $K_{obs} = 0.8 \times 10^6$ M^{-1}.

Table III: Energy Discrimination between GRE and ERE Half-Sites[a]

process	$\Delta\Delta G°_{obs}$ (kcal mol^{-1})
DBD–GREH → DBD–GRE2H	0.4 ± 0.1
DBD–GREH → DBD–EREH/ERE2H	>1.4 ± 0.1
DBD–GRE2H → DBD–EREH/ERE2H	>1.0 ± 0.1

[a] Uncertainties represent estimated standard deviations.

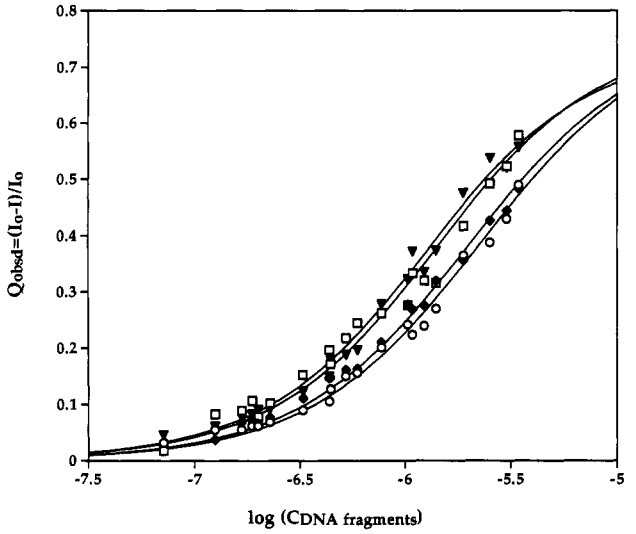

FIGURE 6: Fractional fluorescence quenching as a function of DNA concentration for reverse titrations of GR DBD with GREH at (○) 10, (◆) 12, (□) 15, and (▼) 30 °C at constant protein concentration (0.6 μM). The curves represent the best fit of the theoretical binding isotherm to experimental data with Q_{max} according to Table I. Data points represent the averages with estimated standard deviations of three separate titrations. Buffer conditions are the same as those given in the legend to Figure 3.

cooperative binding by comparing binding to a half-site to that to an idealized GRE with two identical half-sites arranged as inverted repeats; (3) analyze the thermodynamic driving forces for GR DBD binding to a GRE half-site by means of a van't Hoff analysis, i.e., by determining the temperature dependence of the observed equilibrium constant. The buffer conditions used in these studies were carefully chosen to suppress nonspecific binding that occurs at low salt concentrations (Härd et al., 1990a) and in the absence of $MgCl_2$ (not shown). The present buffer conditions also closely approximate those found in the interior of a mammalian cell (Alberts et al., 1983).

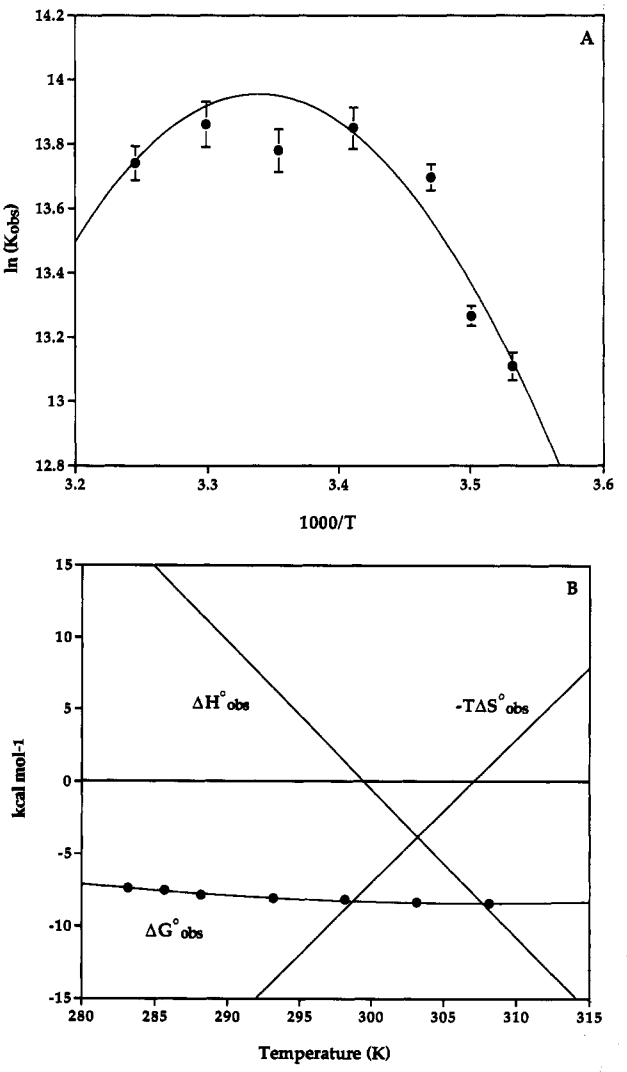

FIGURE 7: (A) Van't Hoff plot of ln K_{obs} versus $1/T$ for GR DBD binding to GREH. The curve represents the best fit of experimental data to eq 2. The error bars represent estimated standard deviations obtained from Monte Carlo simulations as described under Materials and Methods. (B) The thermodynamics of the interaction between GR DBD and GREH showing the change in the nature of thermodynamic driving force with increasing temperature. Experimentally observed $\Delta G°_{obs}$ (●) values in the investigated temperature range are also indicated.

Discrimination between Different Response Elements. The results presented here provide evidence for clearly distinguishable variations in the affinity of the GR DBD to different

nucleotide sequences differing in only one or two base pairs. The free energies for binding to different half-sites, listed in Table III, translate to relative binding affinities that decrease in the order

$$\text{GREH} > \text{GRE2H} > \text{ERE2H} \approx \text{EREH} (\approx \text{CT DNA})$$

These results compare very well to qualitative results obtained from gel-shift experiments on the binding of GR DBD to the corresponding palindromic sequences, where the base pair mutations were made in both half-sites (Zilliacus et al., 1991, 1992).

Independent Measurement of the Cooperativity Parameter. We estimate the cooperativity parameter for dimeric DBD binding to the idealized palindromic GRE to $\omega_{obs} = 25–50$. This result can be compared with our previous studies of GR DBD binding to the GRE from the mouse mammary tumor virus promoter region, where we were able to estimate the product $\omega_{obs}K_{obs} = (1–4) \times 10^7$ M^{-1} at salt concentrations corresponding to 570 mM monovalent cations at pH 7.5 (Härd et al., 1990a). In the previous studies, we also found that the specific binding affinity was relatively independent of salt concentrations in the range 270–570 mM monovalent cations, where the lower value closely corresponds to the buffer conditions used in this study. A problem with the previous studies was that only the product $\omega_{obs}K_{obs}$, where K_{obs} in this case represents the average association constant for binding to two nonequivalent half-site GREs, could be estimated. In the present study, however, we have circumvented this problem by studying binding to an idealized palindromic GRE sequence and by obtaining an independent measure of the binding affinity for a single half-site using the GREH oligomer.

Relative and Absolute DNA Binding Affinities of Intact GR Molecules. The free energy differences for binding to the various half-sites listed in Table III can be related to the expected relative association constants for the binding of the dimerized GR to the corresponding GREs, assuming that the change in free energy for the association with a half-site GRE is the same for intact GR and GR DBD. For instance, the $\Delta\Delta G = -0.4$ kcal mol^{-1} for binding of GR DBD to GREH compared to GRE2H corresponds to $\Delta\Delta G = -0.8$ kcal mol^{-1} for the binding of dimeric GR to GRE versus GRE2, which translates to a 4-fold relative preference for the GRE sequence. The relative binding affinity for GRE versus one of the ERE sequences can in the same way be estimated to >120, i.e., the affinities for the ERE and ERE2 sequences are more than two orders of magnitude less than the affinity for the GRE sequence.

It is also interesting to relate the data obtained with the recombinant GR DBD to the DNA binding affinities measured for the intact GR molecule. It has been suggested that the intact GR binds as a dimer to GRE at natural buffer and GR concentrations, due to additional intermolecular interactions involving regions outside the DBD. The free energy of association of the dimer should be twice that of the monomeric binding, i.e., ΔG(dimeric binding) ≈ -16.2 kcal mol^{-1} at 20 °C (assuming no changes in the interactions between the GR molecules upon binding) which corresponds to an association constant of $>8 \times 10^{11}$ M^{-1}. This value seems unreasonably high considering published association constants for the binding of GR to GRE. For instance, Perlman et al. (1990) studied GR binding to two different (nonpalindromic) GREs at low salt concentrations using quantitative DNase I footprinting and found that the free GR concentration required for 50% occupancy of available binding sites in both cases was $[GR]^{1/2} \approx 2.5 \times 10^{-10}$ M, which is equivalent to a free energy change for dimeric binding of –12.9 kcal mol^{-1} at 20 °C. Thus, if these studies reflect the DNA binding of dimeric receptors, then one has to account for a free energy change of approximately –3.3 kcal mol^{-1} corresponding to the difference between the values calculated here and the values measured by Perlman et al. (1990). Part of the apparent discrepancy probably arises from the fact that the "natural" GRE contains two different half-sites, with a lower affinity of GR to the second half-site. For example, a 10-fold lower affinity to the low-affinity half-site, compared to the high-affinity site studied here, would account for 1.3 kcal mol^{-1}. The fact that the footprinting studies were performed at different buffer conditions might possibly account for some of the remaining discrepancy between the observed and calculated free energy changes. A third possible explanation that could explain the difference would be a destabilization of the GR dimer upon DNA binding. Furthermore, there is evidence indicating that the dimeric form of GR binds with higher affinity to a full-length GRE than the monomeric form (Cairns et al., 1991; Drouin et al., 1992).

An alternative explanation for the large binding constant calculated for the binding of dimeric GR could be that dimerization at low concentrations of GR does not occur prior to DNA binding, but concurrent with DNA binding. The GR is observed to exist as a dimer at total GR concentrations of 0.3 μM (Wrange et al., 1989), suggesting that the GR dimerization constant is at least 10^8 M^{-1}. However, GR is predominantly monomeric at concentrations <1 nM, according to Perlman et al. (1990), proposing that the dimerization constant is $<10^9$ M^{-1}. Considering these numbers, a dimerization upon binding could occur if the GR concentration is in the nanomolar range or less, although it should be noted that the GR dimerization constant might vary somewhat depending on temperature and buffer conditions. The GR probably exists as both monomeric and dimeric species in the cytoplasm, because the concentration of GR in the cytoplasm has been estimated to be in the range of 1–100 nM (Hansson et al., 1981; Gehring et al., 1982). However, if the free GR is monomeric at the conditions at which the footprinting experiments of Perlman et al. (1990) were performed, then the observed free ligand concentration at 50% occupancy of available binding sites would be $[GR]^{1/2} = 1/(K\omega^{1/2})$. [This relationship is easily derived for the two-site cooperative model, e.g., from eq A5 or A6 of Härd et al. (1990a)]. A value of $K_{obs} \approx 10^6$ M^{-1} (as found in this study) would imply that the cooperativity parameter for the binding of intact GR to GRE is $\omega_{GR} \approx 1.6 \times 10^7$, which corresponds to a free energy change of approximately –9.7 kcal mol^{-1} at 20 °C. Using arguments based on a thermodynamic cycle, it can be shown that this change in free energy fits slightly better (the discrepancy is reduced to approximately 1–2 kcal mol^{-1}) to the values obtained for the GR dimerization, without having to invoke effects such as a destabilization of the receptor dimer in the DNA complex. The cooperativity parameter for binding of intact monomeric GR calculated above can be compared to the cooperativity parameter obtained for dimeric binding of the isolated DBD. Such a comparison indicates that a free energy of 7–8 kcal mol^{-1} is gained from protein–protein interactions involving regions outside the DBD.

Origin of the Large ΔC_p for GR DBD Binding to a Half-Site GRE. The graph in Figure 7A indicates the involvement of a large and negative $\Delta C_p^\circ{}_{obs}$ in the association process, which results in highly temperature dependent thermodynamic driving forces, $\Delta H^\circ{}_{obs}$ and $-T\Delta S^\circ{}_{obs}$. These, in turn, almost completely cancel to give a less temperature-dependent change

in free energy, $\Delta G°_{obs}$ (illustrated in Figure 7B). The association process is entropy driven at temperatures below 26 °C and enthalpy driven at temperatures above 35 °C, with an intermediate temperature interval where both enthalpy and entropy contribute. A similar thermodynamic behavior has been observed for the sequence-specific DNA binding of the *lac* repressor and *Eco*RI endonuclease (Ha et al., 1989; Record et al., 1991) and the Cro protein (Takeda et al., 1992), as well as several other procaryotic proteins [reviewed in Record et al. (1991)].

The heat capacity change accompanying any noncovalent process involving a globular protein can be calibrated in terms of the reduction in water-accessible nonpolar surface (the hydrophobic effect) (Spolar et al., 1989; Livingstone et al., 1991), and Ha et al. (1989) argue strongly for dehydration as the major driving force for sequence-specific binding of proteins to DNA. The expected change in $\Delta C_p°_{obs}$ can be calculated from the change in exposed nonpolar surface area (ΔA_{np}) in the protein and DNA upon binding, provided that the hydrophobic effect involved in the association of protein to DNA is equivalent to that observed for protein folding and transferring of nonpolar compounds from water to nonpolar solvents. The binding of GR DBD to DNA provides a good model system for a quantitative test of the contribution of the hydrophobic effect to the observed $\Delta C_p°_{obs}$, because the structures of free DBD and DBD in complex with DNA are known at high resolution from NMR and X-ray crystallographic analyses, respectively. The crystal structure of a DBD–DNA complex has been determined at 2.6-Å resolution (Luisi et al., 1991), and the high-resolution NMR structure of uncomplexed DBD determined in our laboratory (to be published) has a backbone RMSD of ≈0.7 Å (compared to the average structure) for successive distance geometry and simulated annealing calculations. Using these two structures, we calculate $\Delta A_{np} \approx -660$ Å^2 for GR DBD binding to a half-site GRE. This estimate was derived from the accessibility of aliphatic and aromatic carbon and hydrogen atoms using the algorithm of Lee and Richards (1971) within the framework of the CHARMM molecular mechanics package (Brooks et al., 1983). (A similar calculation using the X-ray structure of bound DBD as a reference gives $\Delta A_{np} \approx 760$ Å^2, i.e., there are only minor differences in the accessible surfaces of DBD in the free and bound states). The corresponding contribution to $\Delta C_p°_{obs}$ can then be calculated from $\Delta C_p°_{np} = (-0.33 \pm 0.09)\Delta A_{np} = -0.22 \pm 0.06$ kcal mol^{-1} K^{-1} (Livingstone et al., 1991), which should be compared to the observed $\Delta C_p°_{obs} = 1.0 \pm 0.2$ kcal mol^{-1} K^{-1}. According to Record et al. (1991) and in accordance with our data, all DNA–protein interactions for which $\Delta C_p°_{obs}$ so far has been determined show a larger $\Delta C_p°_{obs}$ than expected from the ΔA_{np} calculated from the complementary surfaces of the protein and DNA. Record et al. (1991) suggest that these observations might be accounted for by changes in protein structure upon DNA binding. However, in the case of GR DBD, where this change can be measured and taken into account, there is still a significant difference between the observed $\Delta C_p°_{obs}$ and the calculated $\Delta C_p°_{np}$. It is possible that cation release (Record et al., 1991, and references therein) might account for a larger contribution than previously thought, or that other effects, such as "stiffening" of vibrational modes or changes in comformational entropy (Sturtevant, 1977), also have to be considered in order to reach a better understanding of the thermodynamics of protein–DNA interactions.

NOTE ADDED IN PROOF

We would like to clarify that Wrange et al. (1989) observe dimeric GR species only after a glutaraldehyde cross-linking reaction. Furthermore, Perlmann et al. (1990) observe a monomeric GR species at 10–20 nM total GR concentrations, rather than <1 nM, as cited in the Discussion. This unfortunate misquotation does not influence the discussion in the remainder of that paragraph, where we assume that the GR is monomeric at the conditions at which the footprinting experiments of Perlmann et al. (1990) were carried out. We would also like to emphasize that Perlmann et al. (1990) present data showing that the free native GR in their binding experiments is largely in a monomeric form, and they also present the two plausible GR dimerization reaction pathways, although their data do not discriminate between the two possibilities.

ACKNOWLEDGMENT

We thank Helmi Siltala for technical assistance in providing purified GR DBD and Dr. Jan-Erik Löfroth for excellent advice regarding the use of nonfluorescent nonionic detergents for use with proteins in solution. We also thank M.Sc. Mats Eriksson for skillful help with computer calculations concerning water-accessible nonpolar surfaces.

SUPPLEMENTARY MATERIAL AVAILABLE

Derivation of the theoretical binding isotherms to the one-site and the two-site models for GR DBD binding to a half-site GRE and a palindromic GRE, respectively (4 pages). Ordering information is given on any current masthead page.

REFERENCES

Alberts, B., Bray, D., Lewis, J., Raff, M., Roberts, K., & Watson, J. D. (1983) in *Molecular Biology of The Cell*, Chapter 6, Garland Publishing, Inc., New York and London.
Beato, M. (1989) *Cell 56*, 335–344.
Berglund, H., Kovács, H., Dahlman-Wright, K., Gustafsson, J.-A., & Härd, T. (1992) *Biochemistry 31*, 12001–12011.
Birdsall, B., King, R. W., Wheeler, M. R., Lewis, C. A., Goode, S. R., Dunlap, R. B., & Roberts, G. C. K. (1983) *Anal. Biochem. 132*, 353–361.
Brooks, B. R., Bruccoleri, R. E., Olafson, B. D., States, D. J., Swaminathan, S., & Karplus, M. (1983) *J. Comput. Chem. 4*, 187–217.
Bulsink, H., Harmsen, B. J. M., & Hilbers, C. W. (1985) *J. Biomol. Struct. Dyn. 3*, 227–247.
Cairns, W., Cairns, C., Pongratz, I., Poellinger, L., & Okret, S. (1991) *J. Biol. Chem. 266*, 11221–11226.
Cantor, C. R., & Schimmel, P. R. (1980) in *Biophysical Chemistry*, Part II, Freeman, San Francisco.
Dahlman-Wright, K., Siltala-Roos, H., Carlstedt-Duke, J., & Gustafsson, J.-A. (1990) *J. Biol. Chem. 265*, 14030–14035.
Dahlman-Wright, K., Wright, A., Gustafsson, J.-A., & Carlstedt-Duke, J. (1991) *J. Biol. Chem. 266*, 3107–3112.
Danielsen, M., Hinck, L., & Ringold, G. M. (1989) *Cell 57*, 1131–1138.
Drouin, J., Jin Sun, Y., Tremblay, S., Javender, P., Schmidt, T. J., de Jean, A., & Nemer, M. (1992) *Mol. Endocrinol. 6*, 1299–1309.
Evans, R. M. (1988) *Science 240*, 889–895.
Gehring, U., Spindler-Barth, N., & Ulrich, J. (1982) *Biochem. Biophys. Res. Commun. 108*, 627–634.
Ha, J.-H., Spolar, R. S., & Record, M. T. (1989) *J. Mol. Biol. 209*, 801–816.
Hansson, L.-A., Gustafsson, S. A., Carlstedt-Duke, J., Gahrton, G., Högberg, B., & Gustafsson, J.-A. (1981) *J. Steroid. Biochem. 14*, 757–764.

Härd, T., Dahlman, K., Carlstedt-Duke, J., Gustafsson, J.-A., & Rigler, R. (1990a) *Biochemistry 29*, 5358–5364.
Härd, T., Kellenbach, E., Boelens, R., Maler, B. A., Dahlman, K., Freedman, L. P., Carlstedt-Duke, J., Yamamoto, K. R., Gustafsson, J.-A., & Kaptein, R. (1990b) *Science 249*, 157–160.
Härd, T., Kellenbach, E., Boelens, R., Kaptein, R., Dahlman, K., Carlstedt-Duke, J., Freedman, L. P., Maler, B. A., Hyde, E. I., Gustafsson, J.-A., & Yamamoto, K. R. (1990c) *Biochemistry 29*, 9015–9023.
Lee, B., & Richards, F. M. (1971) *J. Mol. Biol. 55*, 379–400.
Livingstone, J. R., Spolar, R. S., & Record, M. T. (1991) *Biochemistry 30*, 4237–4244.
Luisi, B. F., Xu, W. X., Otwinowski, Z., Freedman, L. P., Yamamoto, K. R., & Sigler, P. B. (1991) *Nature 352*, 497–505.
Mader, S., Kumar, V., de Verneuil, H., & Chambon, P. (1989) *Nature 338*, 271–274.
Mahler, H. R., Kline, B., & Mehrota, B. D. (1964) *J. Mol. Biol. 9*, 801–811.
Marshall, A. G. (1978) in *Biophysical Chemistry*, Chapter 3, John Wiley & Sons, New York.
Pabo, C. O., & Sauer, R. T. (1992) *Annu. Rev. Biochem. 61*, 1053–1095.
Perlmann, T., Eriksson, P., & Wrange, Ö. (1990) *J. Biol. Chem. 265*, 17222–17229.
Press, W. H., Flannery, B. P., Teukolsky, S. A., & Vetterling, W. T. (1986) in *Numerical Recipes*, Chapter 14, Cambridge University Press, Cambridge, England.
Record, M. T., Ha, J.-H., & Fisher, M. A. (1991) *Methods Enzymol. 208*, 291–343.
Schwabe, J. W., Neuhaus, D., & Rhodes, D. (1990) *Nature 348*, 458–461.
Spolar, R. S., Ha, J.-H., & Record, M. T. (1989) *Proc. Natl. Acad. Sci. U.S.A. 86*, 8382–8385.
Strähle, U., Klock, G., & Schütz, G. (1987) *Proc. Natl. Acad. Sci. U.S.A. 84*, 7871–7875.
Sturtevant, J. M. (1977) *Proc. Natl. Acad. Sci. U.S.A. 74*, 2236–2240.
Takeda, Y., Ross, P. D., & Mudd, C. P. (1992) *Proc. Natl. Acad. Sci. U.S.A. 89*, 8180–8184.
Tsai, S. Y., Carlstedt-Duke, J., Weigel, N. L., Dahlman, K., Gustafsson, J.-A., Tsai, M.-J., & O'Malley, B. W. (1988) *Cell 55*, 361–369.
Umesono, K., & Evans, R. M. (1989) *Cell 57*, 1139–1146.
Wrange, Ö., Eriksson, P., & Perlmann, T. (1989) *J. Biol. Chem. 264*, 5253–5259.
Zilliacus, J., Dahlman-Wright, K., Wright, A., Gustafsson, J.-A., & Carlstedt-Duke, J. (1991) *J. Biol. Chem. 266*, 3101–3106.
Zilliacus, J., Wright, A. P. H., Norinder, U., Gustafsson, J.-A., & Carlstedt-Duke, J. (1992) *J. Biol. Chem. 267*, 24941–24947.